

Coordination Chemistry | Hot Paper |

Tricoordinate Coinage Metal Complexes with a Redox-Active Tris-(Ferrocenyl)triazine Backbone Feature Triazine–Metal Interactions

Axel Straube,^[a] Peter Coburger,^[a, c] Mark R. Ringenberg,^[b] and Evamarie Hey-Hawkins^{*[a]}

Abstract: 2,4,6-Tris(1-diphenylphosphanyl-1'-ferrocenyl)-1,3,5-triazine (**1**) coordinates all three coinage metal(I) ions in a 1:1 tridentate coordination mode. The C_3 -symmetric coordination in both solid state and solution is stabilised by an uncommon cation– π interaction between the triazine core and the metal cation. Intramolecular dynamic behaviour was observed by variable-temperature NMR spectroscopy. The borane adduct of **1**, **1BH₃**, displays four accessible oxidation states, suggesting complexes of **1** to be intriguing candidates for redox-switchable catalysis. Complexes **1Cu**, **1Ag**, and **1Au** display a more complicated electrochemical behaviour, and the electrochemical mechanism was studied by temperature-resolved UV/Vis spectroelectrochemistry and chemical oxidation.

Over the past decades, C_3 symmetry has been an intriguing structural feature in ligand design, providing transition-metal complexes with increased stability and minimising the possible number of transition states especially in the context of asymmetric homogeneous catalysis.^[1] One trend in modern-day ligand design is to incorporate redox-switchable units into existing ligand frameworks or to design de novo potential ligands featuring such groups. This method has paved the way for redox-switchable catalysis (RSC).^[2] Embedded into the greater field of “smart”, that is, stimuli-responsive catalysts,^[3] RSC is of particular interest in the context of catalyst recycling and orthogonal reactivity for building complex molecular structures. Among the available structural motifs, ferrocenyl

groups have found the most widespread use in this field, owing to their highly reversible redox processes, their structural flexibility, and their amenability to many different synthetic procedures.^[4] Combining both approaches and downsizing our recently reported redox-switchable dendritic ferrocenyl-based catalysts,^[5] our present work aims to utilise the structurally appealing C_3 -symmetric 1,3,5-tris(ferrocenyl)arene platform^[6] (some examples are shown in Figure 1) for the design of stimuli-responsive ligands. Having been extensively studied for their electrochemistry (**IV**, **VI**, **VII**) and, to some degree, suitability for nonlinear optics (**II**, **V**), these molecules—in themselves promising candidates for molecular materials as redox-active build-

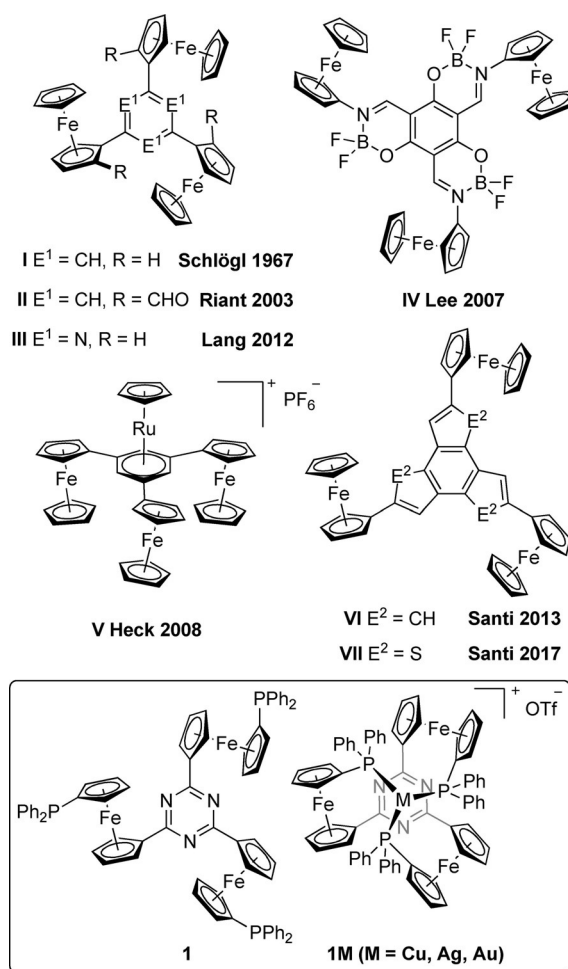


Figure 1. C_3 -symmetric tris(ferrocenyl)arenes documented in the literature and presented in this work (box, bottom).

[a] A. Straube, Dr. P. Coburger, Prof. Dr. E. Hey-Hawkins
Institute of Inorganic Chemistry, Universität Leipzig
Johannisallee 29, 04103 Leipzig (Germany)
<https://anorganik.chemie.uni-leipzig.de/anorganik/ak-hey-hawkins/>
E-mail: hey@uni-leipzig.de

[b] Dr. M. R. Ringenberg
Institute of Inorganic Chemistry, Universität Stuttgart
Pfaffenwaldring 55, 70569 Stuttgart (Germany)

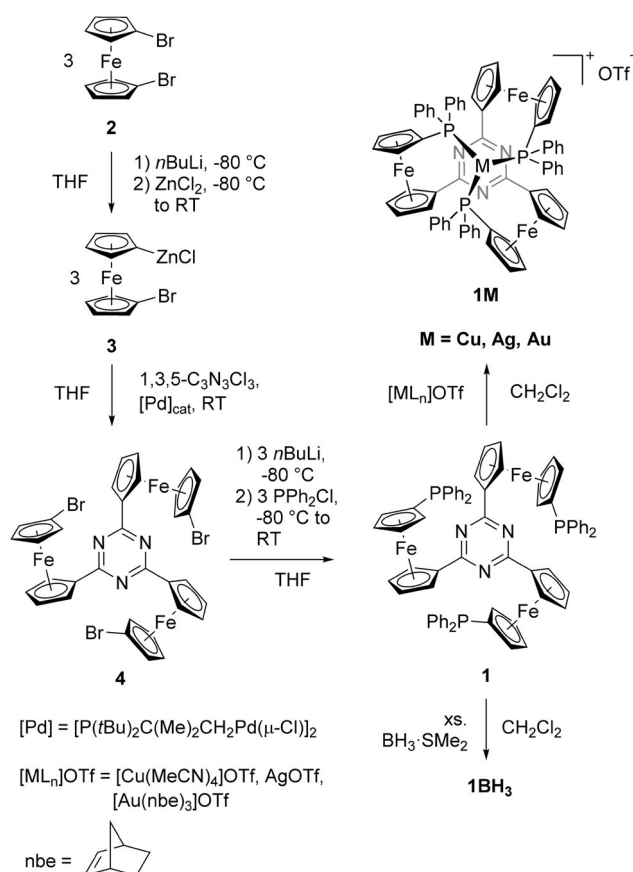
[c] Dr. P. Coburger
Present address: Institute of Inorganic Chemistry, Universität Regensburg
Universitätsstraße 31, 93051 Regensburg (Germany)

Supporting information and the ORCID identification numbers for the authors of this article can be found under:
<https://doi.org/10.1002/chem.202000226>.

© 2020 The Authors. Published by Wiley-VCH Verlag GmbH & Co. KGaA. This is an open access article under the terms of the Creative Commons Attribution License, which permits use, distribution and reproduction in any medium, provided the original work is properly cited.

ing blocks—have not yet found their way into coordination chemistry with the notable exception reported by the Heck group, who used the central benzene core of **1** as η^6 -coordinating ligand in **V**.^[6d]

Therefore, we prepared tris-phosphane **1** in a modular two-step procedure from 1,1'-dibromoferrocene (**2**)^[7] and cyanuric chloride (Scheme 1, left), noting that other arene cores can be utilised at this stage. Adapting a procedure from the Lang group for **III**,^[6e] 2,4,6-tris(1-bromo-1'-ferrocenylene)-1,3,5-triazine (**4**) was obtained in good yield through a Negishi cou-



Scheme 1. Preparation of tris-phosphane **1** and its corresponding coinage metal complexes **1Cu**, **1Ag**, and **1Au**. Isolated yields are given in brackets.

pling reaction and, after chromatographic purification, was further reacted with chlorodiphenylphosphane. **4** provides an intriguing starting point for the preparation of complex structures based on the tris(ferrocenyl)arene scaffold. The resulting tris-phosphane **1** and its borane adduct (**1BH₃**) were fully characterised, including their solid-state structures by single-crystal X-ray crystallography (XRD) (see Supporting Information).

In the solid state, **1** exhibits an all-*syn* conformation, contrasting the C_{3v} symmetry in solution assessed by NMR spectroscopy and, thus, implying free rotation of the C_3N_3 -ferrocenylene bonds. This prompted us to investigate the eligibility of this molecule for a tricoordinate binding mode towards coinage metal(I) ions, given their propensity for low coordination numbers and flexibility regarding their coordination geometry due to their closed-shell d^{10} electronic configurations.^[8]

Accordingly, **1** was reacted with suitable metal(I) triflate precursors in dichloromethane (Scheme 1, right). The corresponding 1:1 (metal-to-ligand) complexes **1Cu**, **1Ag**, and **1Au** were formed instantaneously, as shown by $^{31}\text{P}\{^1\text{H}\}$ NMR spectroscopy. They can be easily isolated as moderately air-stable crystals in good yields. Crystals grown from dichloromethane/toluene (**1Cu**) or from 1,2-dichloroethane/toluene (**1Ag**, **1Au**) proved suitable for XRD, allowing to ascertain the desired tricoordinate binding mode in the solid state (Figure 2).

According to the XRD data, the three complexes form close-to-isomorphous crystals (space group $P\bar{1}$), minor deviations in their cell parameters arising from anions and (disordered) solvent molecules (see Supporting Information). No contacts between the metal ions and their respective triflate anions are present. There are no noteworthy differences between the three ferrocenyl moieties; thus, only average values are listed (Table 1). The coinage metal ions adopt an almost ideal trigonal-planar coordination environment with a small deflection of the metal from its position in an idealised P_3P_3 plane towards the triazine core (distance d in Table 1), also causing the deviations from the ideal 120° bond angles. The average M–P bond lengths are in line with the differences in the covalent radii of the metal ions.^[9] For **1Ag** and **1Au**, the absolute values are well within the reported range for trigonal-planar tris-phosphane complexes of silver(I) and gold(I), a structural motif still found to be quite rare among compounds published in the

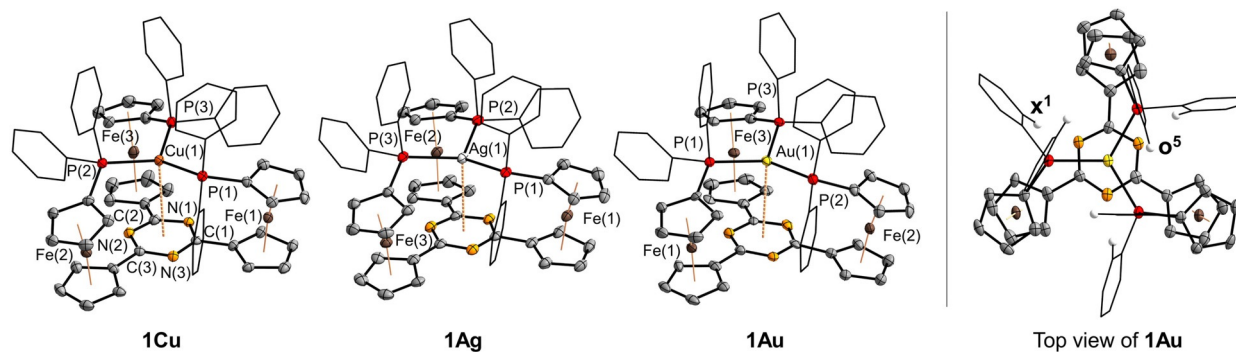


Figure 2. Molecular structures of coinage metal complexes of **1** and top view of **1Au** showcasing the propeller-like arrangement of the complexes as well as two types of phenyl protons (x^1 and o^5) in spectroscopically relevant positions. Thermal ellipsoids are set at the 50% probability level. For clarity, the phenyl rings are drawn as wireframes, the triflate anions have been omitted, and hydrogen atoms except for x^1 and o^5 are not depicted.

Table 1. Selected average bond lengths [Å], distances [Å], and angles [°] of complexes 1Cu , 1Ag , and 1Au .			
	1Cu	1Ag	1Au
P–M(1)	2.3261(7)	2.4910(6)	2.396(2)
C ₃ N ₃ ⋯M(1) ^[a]	3.599	3.430	3.571
d ^[b]	0.297	0.382	0.299
P _a –M(1)–P _b	118.38(3)	117.69(2)	118.46(6)
γ ^[c]	1.35	1.10	0.287
α ^[d]	172.68	173.22	173.11
θ ^[e]	7.48	6.91	7.45
τ ^[f]	22.19	24.20	23.38

[a] Distance between a calculated C₃N₃ centroid and M(1). [b] Distance between M(1) and a plane defined by P(1), P(2), and P(3). [c] Angle between axis C₃N₃⋯M(1) and vector normal to the C₃N₃ plane. [d] Average tilt angle about Cp^P(centroid)⋯Fe⋯Cp^C(centroid) axes. [e] Average angle between mean planes through cyclopentadienyl (Cp^R) rings. [f] Average torsion about the Cp^P(centroid)⋯Fe⋯Cp^C(centroid) axes. See the Supporting Information for a graphic representation of the geometric parameters.

Cambridge Structural Database (CSD),^[10] particularly when only 1:1 complexes are considered. In the case of **1Cu**, the Cu–P bonds are among the longest that have been reported for this coordination mode (see the Supporting Information for a full list of 1:1 coinage metal-tris-phosphane complexes). Ligand **1** thus constitutes only the second example for a tris-phosphane capable of binding all coinage metal ions in the same trigonal-planar coordination mode without an additional ligand, as in tris[2-(diphenylphosphino)ethyl]amine (NP₃) complexes **VIII** (Figure 3).^[11]

A tris-phosphino-borane by Bourissou and co-workers coordinates the coinage metal chlorides (complexes **IX**),^[12] with the Z-type boron–metal interactions persisting upon chloride abstraction for gold(I) and copper(I).^[13] In these selected exam-

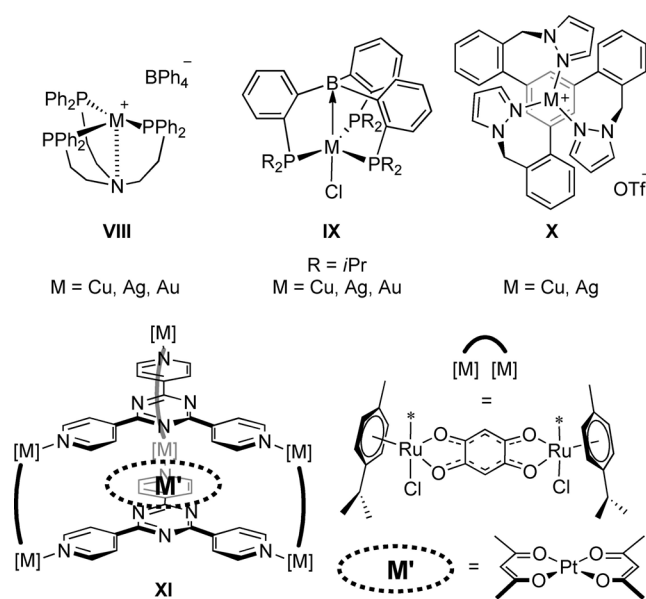


Figure 3. Selected examples of coordination compounds with trigonal-planar coinage metal ions (**VIII–X**) and arene(**X**)/C₃N₃(**XI**)⋯M^I contacts.

ples, the metal ions are in close contact with an additional donor atom (**VIII**) or a Z-type acceptor group (**IX**). Broadening the ligand scope, similar complexes of a tris(pyrazoly) ligand with copper(I) and silver(I), **X**,^[14] feature an interaction with the central arene core. Indeed, most trigonal-planar 1:1 coinage metal complexes and all of those based on tris-phosphanes generally feature such contacts, including metallophilic interactions,^[15] which could thus be considered a requirement. In analogy to **VIII**, **IX**, and **X**, complexes **1M** crystallise in a helically twisted, propeller-like arrangement (Figure 2, right), represented by the synclinal conformation ($\tau = 22.19^\circ$ – 24.20°) of the ferrocenylene groups,^[16] both enantiomers (*P* and *M*) are present in the unit cell as evident from the space group (*P* $\bar{1}$; see Supporting Information for a packing diagram of **1Au**).

In the case of triazine, the observed close, intramolecular C₃N₃⋯M^I contacts, combined with the almost perfect centring of the metal (signified by angle γ , Table 1) and classified as delocalised M⋯ π (arene) interactions for gold by Tiekink,^[17] are still rare. For other, more electron-rich arenes, close contacts between (coinage) metals and the ring system have been found to be important structural motifs with potential impact on catalytic activities.^[17,18] Even though 1,3,5-triazine has recently been recognised as a hybrid system capable of binding both cations and anions,^[19] only the latter has been exploited in many examples,^[20] while the former has mainly been investigated in silico for the alkaline metals.^[21] Complexes **1M**, reported here, show the closest C₃N₃⋯M^I distance for both copper(I) and silver(I). In the case of gold(I), a shorter (3.511 Å), yet intermolecular and less well-centred contact ($\gamma = 10.7^\circ$) has been reported before.^[22]

Among all metals, these distances are only underbid by bis-(acetylacetonato)platinum(II) and -palladium(II) encapsulated in a C₃-symmetric molecular clip **XI** (Figure 3, C₃N₃⋯Pt = 3.397 Å, $\gamma = 2.9^\circ$)^[23] and a less well-centred nickel(II) analogue.^[24] The authors, however, only stated aromatic π – π interactions as the main reason for the successful encapsulation of both complexes. The reader is referred to the Supporting Information for a survey of such structures in the CSD. Computational methods were employed in order to gain more insight into the nature of the C₃N₃⋯M^I (M = Cu, Ag, Au) interaction. As expected and previously noted on interactions between triazine and sodium cations,^[21a] the triazine core serves as an additional donor for the metal(I) ions. Studying the interaction of the metal with the parent triazine C₃H₃N₃ (see Supporting Information), EDA-NOCV analyses furthermore show polarisation of the triazine framework to significantly (20–23%) contribute to the overall interaction energies. The Wiberg bond indices reveal weak interactions between the metals and the triazine core in the order (Ag > Au > Cu), the order also found for the C₃N₃⋯M^I distances of the complexes in their molecular structures.

Despite their striking similarity in the solid state, the behaviour of the complexes in CH₂Cl₂ turned out to be markedly different. While solutions of **1Ag** and **1Au** display only one ³¹P resonance, **1Cu** yields two ³¹P resonances at –7.3 ppm and –20.4 ppm (2:1), suggesting only two phosphanyl groups to be involved in the bonding of the Cu^I ion and in contradiction to its solid-state structure. Similarly, the signals in the room-

temperature ^1H NMR spectra of the three complexes are broadened (most strongly for **1Ag**), and, in the case of **1Cu**, are neither in line with the solid-state structure nor the finding from the $^{31}\text{P}\{^1\text{H}\}$ NMR spectrum. We assumed fast interconversion of the two helical isomers of **1Ag** and **1Au**, as reported for **IX** at elevated temperatures, to be responsible for the line broadening and apparent C_{3v} symmetry in solution at and above room temperature.

Variable-temperature (VT) NMR experiments were thus conducted in CD_2Cl_2 between 40°C and -70°C . Both the C_{3v} -symmetric ^1H NMR spectrum of **1Au** (Figure 4, bottom left) and the severely broadened signals in the ^1H NMR spectrum of **1Ag** sharpen in linewidth and break down into apparent C_3 symmetry [$T_{\text{coal}}(\mathbf{1Ag}) = 248 \pm 5 \text{ K}$, $T_{\text{coal}}(\mathbf{1Au}) = 268 \pm 5 \text{ K}$], rendering all eight ferrocenylene protons distinguishable (Figure 4, left). Most strikingly, the phenyl protons decoalesce and span the region from 5.8 ppm to 9.7 ppm, the most deshielded signal corresponding to the phenyl protons \mathbf{x}^1 buried between the two ferrocenylene units and the most shielded signal to the protons \mathbf{o}^5 closest to the gold(I) ion (Figure 2, right; Figure 4, bottom left), the latter in line with findings from the Mingos group.^[25] ^1H , ^1H COSY NMR experiments conducted at -50°C for **1Au** as well as NMR shielding parameters obtained from DFT calculations support this assignment, and the $^{31}\text{P}\{^1\text{H}\}$ VT NMR spectra agree with these findings.

The low-temperature ^1H NMR spectrum of **1Cu** (Figure 4, middle left) exhibits signals of both a C_3 -symmetric form **1Cu_{cl}** and an open form **1Cu_{op}** with C_1 symmetry (Figure 4, bottom right), featuring 24 partly overlapping signals for the ferrocenylene protons. Both forms are in a slow equilibrium, thus observable on the NMR timescale.

Likewise, the $^{31}\text{P}\{^1\text{H}\}$ NMR spectrum of **1Cu** at -70°C (Figure 4, top left) consists of three signals; one sharp singlet at -14.2 ppm corresponding to the three Cu^{I} -bound phosphanyl moieties of **1Cu_{cl}**, a second singlet at -23.2 ppm , and a higher-order AB multiplet at -7.9 ppm in the intensity ratio of 1:2, thus corresponding to **1Cu_{op}**. The respective $^2J_{\text{PP}}$ coupling constant of 122 Hz is in line with previously reported values^[26] and constitutes a rare example of a resolved, Cu^{I} -mediated $^2J_{\text{PP}}$ coupling in solution,^[27] mostly only being measurable by ^{31}P CP-MAS NMR studies in the solid state.^[28] In order to understand whether this behaviour is connected to the triflate anion—copper(I) is known to bind triflates in the solid state^[29]—two different Cu^{I} complexes containing tetrafluoroborate **1CuBF₄** and tetrakis(3,5-bis(trifluoromethyl)phenyl)borate (BARF_4^-) anions **1CuBARF₄** were prepared and characterised, including their molecular structures in the solid state; no significant changes in the cation structural parameters were observed (see Supporting Information). The VT NMR spectra of **1CuBF₄** and **1CuBARF₄** in CD_2Cl_2 match those of **1Cu** very closely, and no peak splitting or broadening is observed for both the ^{11}B and ^{19}F NMR signals at low temperatures, suggesting no anion involvement in the equilibrium between **1Cu_{cl}** and **1Cu_{op}** in CD_2Cl_2 . Most likely and also observable in a hypothetical structure for **1Cu_{op}** obtained from a DFT calculation (see Supporting Information), coordination of Cu^{I} by the C_3N_3 core^[30] is present in the open form **1Cu_{op}**. A bidentate form has also been proposed as the intermediate for the helical interconversion in a dissociative pathway by Bourissou and co-workers.^[12]

UV/Vis spectroscopy supports this notion; since the transition centred at 500 nm is mainly of $d(\text{Fe})-\pi^*(\text{C}_3\text{N}_3)$ character (cf.

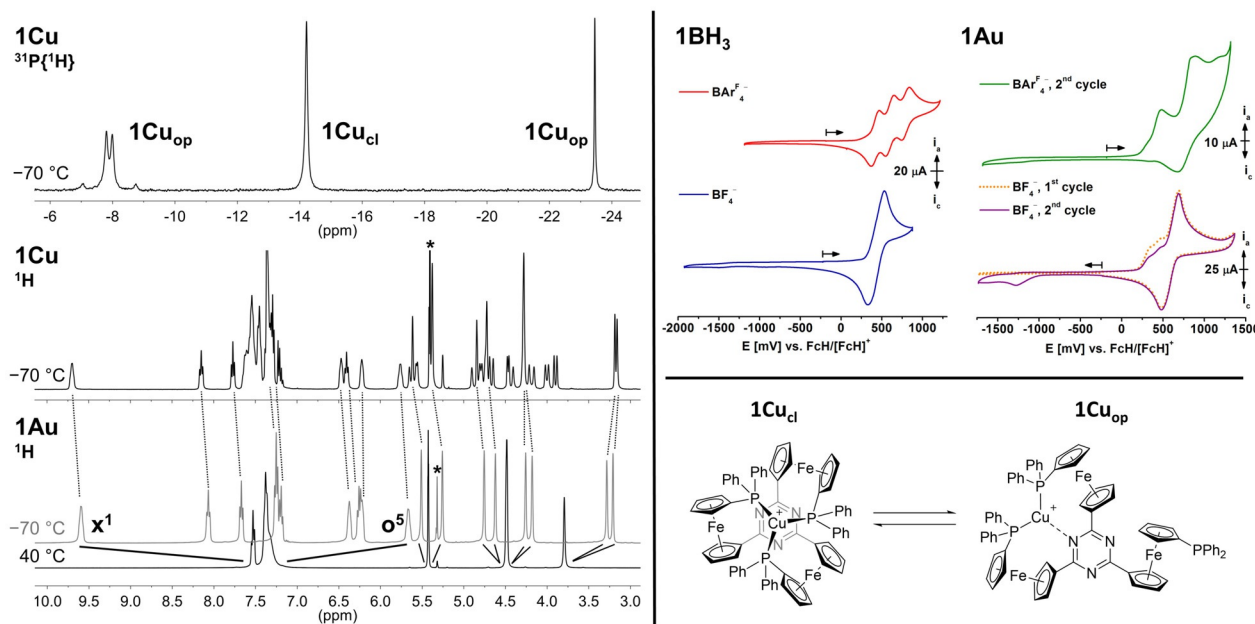


Figure 4. Left: VT ^1H and $^{31}\text{P}\{^1\text{H}\}$ NMR spectra of **1Cu** and **1Au** at 40°C and -70°C ; the asterisk denotes the CH_2Cl_2 signal, \mathbf{x}^1 and \mathbf{o}^5 denote signals of interest (see also Figure 2, right). Solid lines represent the signal splitting, and dashed lines link analogous signals of **1Cu_{cl}** and **1Au**. Top right: Cyclic voltammograms of **1BH₃** and **1Au** in the BF_4^- - and BARF_4^- -based SE; arrows denote the starting potential and initial scan direction at 100 mV s^{-1} . The second of three consecutively measured cycles is shown if not noted otherwise. Bottom right: Equilibrium between two coordination isomers of **1Cu** in solution.

Supporting Information), bound Cu^I will strongly affect it, explaining the bathochromic shift and peak broadening observed between **1Cu** and **1Au** ($\Delta\lambda_{\text{max}} = 15$ nm) as both compounds **1Cu** and **1Au** are practically identical in the solid state. Among **1M**, only **1Cu** shows a pronounced solvent influence on its NMR and UV/Vis spectra, indicative of the lability of the C₃N₃-Cu contact in coordinating solvents. A UV/Vis-titration of **1Cu** in CH₂Cl₂ with up to 2 equiv of CN⁻ further underpins this hypothesis (see Supporting Information).

Given our aim to utilise these complexes in RSC, their electrochemical characterisation by cyclic voltammetry (CV) was of great interest. Tris(ferrocenyl)triazine **III** itself had already been studied by the group of Lang and showed three separate, resolved oxidation waves in the CV when very weakly coordinating supporting electrolytes (SE), such as (*n*Bu₄N)[B(C₆F₅)₄], were used.^[6e] Through UV/Vis spectroelectrochemical analyses, Lang and co-workers could further demonstrate that mono- and di-oxidised **III** have localised charges (Robin–Day class I), in contrast to other oxidised di- and tri(ferrocenyl)arenes.

The CV recorded in the BARF₄⁻-based SE showed that the precursor **2** shows similar, anodically shifted redox potentials as **III** due to the presence of the bromine substituents, and one singular reversible redox wave in (*n*Bu₄N)BF₄ as the SE. The free ligand **1** can only be irreversibly oxidised during cyclic voltammetry in both SEs, in line with previous reports for ferrocenylphosphanes.^[31] In contrast, its borane-protected analogue **1BH₃** again allows for threefold oxidation in the BARF₄⁻-based SE, proving the principal suitability of **1** for a four oxidation-state catalyst system for RSC (Figure 4, top right).

The investigation of the electrochemical features of complexes **1M** by CV (exemplarily shown for **1Au** in Figure 4, top right) turned out to be less straightforward. None of **1M** exhibits a single, reversible redox wave in the BF₄⁻- or the BARF₄⁻-based SE. In the former, all complexes display an irreversible first oxidation step at 250–350 mV vs. FcH/[FcH]⁺, followed by further oxidation events. Linked to the first oxidation(s), one or two scan speed-dependent reduction steps at much more cathodic potentials (**1Cu**: -1.4 V, **1Ag**: -450 mV and -1.3 V, **1Au**: -1.3 V vs. FcH/[FcH]⁺) hint at an electron transfer-induced chemical reaction (EC) mechanism in which step C might involve a geometric rearrangement or an intramolecular electron transfer, producing a species [1Au]^{ox} which is more difficult to reduce.^[32] The complexes behave similar in the BARF₄⁻-based SE, even though the delayed reductions are less prominent, particularly for **1Au** (Figure 4, top right).

To gain further understanding, spectroelectrochemical measurements were conducted in the BARF₄⁻-based SE (Figure 5, left). At 25 °C and at -50 °C, the first oxidation of **1Au** yields a species [1Au]^{ox} that is reducible again to form [1Au]^x.

The UV/Vis spectrum of [1Au]^x does however not match that of **1Au** (cf. Supporting Information). In contrast, performing the first oxidation at -80 °C results in the appearance of a markedly different UV/Vis spectrum with almost full reversibility upon reduction. The UV/Vis signature relates to an Fe-centred oxidation [1Au]^{ox1},^[33] in line with DFT analyses finding the HOMO of **1Au** to be located at the ferrocenyl moieties (see Supporting Information). A second oxidation at -80 °C and

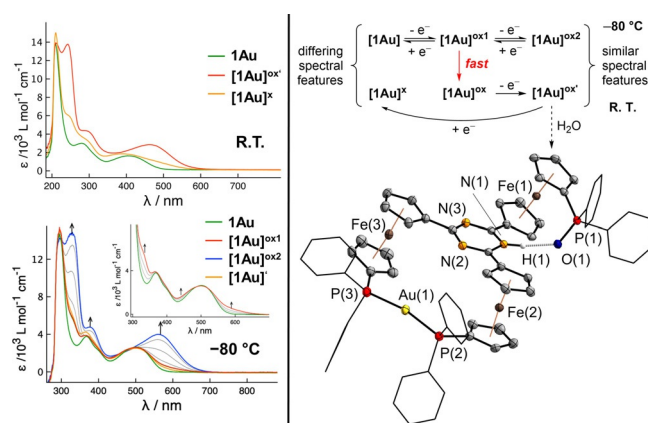
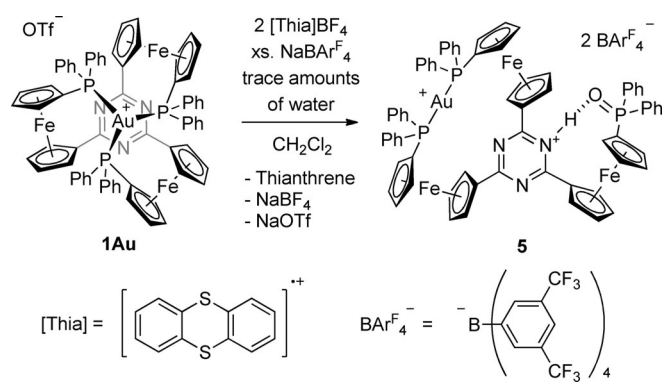


Figure 5. Left: UV/Vis SEC of **1Au** in 0.1 M (*n*Bu₄N)BARF₄⁻ in CH₂Cl₂, recorded at room temperature (top, intermediate spectra omitted for clarity) and at -80 °C (bottom, insert highlighting the first intermediate process). Right: Electrochemistry of **1Au** as assessed by VT SEC (top) and molecular structure of oxidation product **5**. Thermal ellipsoids are set at the 50% probability level. For clarity, the phenyl rings are drawn as wireframes, the two BARF₄⁻ anions have been omitted, and hydrogen atoms except for H(1) are not depicted. For structural parameters, see the Supporting Information.

higher potential generates a species [1Au]^{ox2} with the same spectral features as [1Au]^{ox} generated from oxidising **1Au** at room temperature (see Supporting Information). We thus conclude that **1Au** is indeed oxidised following an EC mechanism in which the chemical reaction, fast at temperatures above -80 °C, transforms [1Au]^{ox1} into an easier-to-oxidise species (Figure 5, top right) that is immediately oxidised further to [1Au]^{ox}/[1Au]^{ox2}. Similar observations have been made for **1Cu**, whereas at -80 °C **1Ag** is showing the same characteristics as **1Au** at -50 °C (cf. Supporting Information).

In an attempt to isolate and characterise [1Au]^{ox} by chemical oxidation using two equivalents [thianthrenium]BARF₄ (Scheme 2), a few crystals of a dicationic, dicoordinate gold complex **5**, protonated at the triazine core and bearing a phosphine oxide moiety at the third ferrocenyl group (Figure 5, bottom right), were isolated.

Adventitious traces of water likely react with the highly reactive species [1Au]^{ox}—most likely a P-centred radical formed after de-coordination of one phosphanyl group^[34]—to form



Scheme 2. Chemical oxidation of **1Au** using [thianthrenium]BARF₄ in the presence of an excess of NaBARF₄ to yield oxidised product **5**.

this product in a formal oxidation from P^{III} to P^V, further underpinning the proposed EC mechanism.

In summary, we have prepared the first tridentate ligand based on a C₃-symmetric tris(ferrocenyl)arene scaffold, **1**, and the corresponding coinage metal(I) complexes. The rare, C₃N₃-supported and almost perfectly trigonal-planar tricoordinate binding mode for all three coinage metal ions is tied to helical interconversion at low temperatures. While the borane adduct **1BH₃** can be triply oxidised in a stepwise fashion, mononuclear complexes **1M** display a temperature-dependent oxidation behaviour linked to an EC mechanism. Mono- and multinuclear complexes of **1** are intriguing candidates for RSC, and corresponding experiments are currently being carried out in our laboratories.

Experimental Section

Crystallographic data: CCDC 1960989 (**1**), 1960985 (**1BH₃**), 1960986 (**1Cu**), 1960991 (**1CuBF₄**), 1960987 (**1CuBAr^F₄**), 1960992 (**1Ag**), 1960988 (**1Au**), and 1960990 (**5**) contains the supplementary crystallographic data for this paper. These data can be obtained free of charge from The Cambridge Crystallographic Data Centre.

Acknowledgements

Financial support by the Studienstiftung des deutschen Volkes (doctoral fellowships to A.S. and P.C.) is gratefully acknowledged. M.R.R. gratefully acknowledges funding provided by the Universität Stuttgart, Stuttgart DE. The authors thank Dr. Eckhard Bill (MPI CEC, Mülheim (Ruhr)) for supporting EPR and Mössbauer spectroscopy measurements and Prof. Rainer Winter and M.Sc. Nils Rotthowe (Universität Konstanz) for recording the room temperature-SEC spectra of **1Au**.

Conflict of interest

The authors declare no conflict of interest.

Keywords: coinage metal ions · ligand design · phosphane ligands · π interactions · tridentate ligands

- [1] a) C. Moberg, *Angew. Chem. Int. Ed.* **1998**, *37*, 248–268; *Angew. Chem.* **1998**, *110*, 260–281; b) S. E. Gibson, M. P. Castaldi, *Angew. Chem. Int. Ed.* **2006**, *45*, 4718–4720; *Angew. Chem.* **2006**, *118*, 4834–4837.
- [2] a) A. M. Allgeier, C. A. Mirkin, *Angew. Chem. Int. Ed.* **1998**, *37*, 894–908; *Angew. Chem.* **1998**, *110*, 936–952; b) M. Süßner, H. Plenio, *Angew. Chem. Int. Ed.* **2005**, *44*, 6885–6888; *Angew. Chem.* **2005**, *117*, 7045–7048; c) A. G. Tennyson, V. M. Lynch, C. W. Bielawski, *J. Am. Chem. Soc.* **2010**, *132*, 9420–9429.
- [3] a) V. Blanco, D. A. Leigh, V. Marcos, *Chem. Soc. Rev.* **2015**, *44*, 5341–5370; b) J. Choudhury, *Tetrahedron Lett.* **2018**, *59*, 487–495.
- [4] a) *Ferrocenes, Homogeneous Catalysis, Organic Synthesis Materials Science* (Eds.: A. Togni, T. Hayashi), Wiley-VCH, Weinheim, **1995**; b) P. Štěpnička (Ed.), *Ferrocenes, Ligands, Materials and Biomolecules*, Wiley, Chichester, **2008**; c) D. Astruc, *Eur. J. Inorg. Chem.* **2017**, 6–29.
- [5] a) P. Neumann, H. Dib, A.-M. Caminade, E. Hey-Hawkins, *Angew. Chem. Int. Ed.* **2015**, *54*, 311–314; *Angew. Chem.* **2015**, *127*, 316–319; b) P. Neumann, H. Dib, A. Sourmia-Saquet, T. Grell, M. Handke, A.-M. Caminade, E. Hey-Hawkins, *Chem. Eur. J.* **2015**, *21*, 6590–6604.
- [6] a) K. Schlögl, H. Soukup, *Tetrahedron Lett.* **1967**, *8*, 1181–1184; b) V. Mamane, I. Ledoux-Rak, S. Deveau, J. Zyss, O. Riant, *Synthesis* **2003**, *3*, 0455–0467; c) Y.-K. Lim, S. Wallace, J. C. Bollinger, X. Chen, D. Lee, *Inorg. Chem.* **2007**, *46*, 1694–1703; d) S. Steffens, M. H. Prosenc, J. Heck, I. Asselberghs, K. Clays, *Eur. J. Inorg. Chem.* **2008**, 1999–2006; e) U. Pfaff, A. Hildebrandt, D. Schaarschmidt, T. Hahn, S. Liebing, J. Kortus, H. Lang, *Organometallics* **2012**, *31*, 6761–6771; f) A. Donoli, A. Bisello, R. Cardena, C. Prinziavalli, S. Santi, *Organometallics* **2013**, *32*, 1029–1036; g) S. Alvarez, *Dalton Trans.* **2013**, *42*, 8617–8636; h) S. Rossi, A. Bisello, R. Cardena, L. Orian, S. Santi, *Eur. J. Org. Chem.* **2017**, 5966–5974; i) S. Rossi, A. Bisello, R. Cardena, S. Santi, *Organometallics* **2018**, *37*, 4242–4249.
- [7] M. S. Inkpen, S. Du, M. Driver, T. Albrecht, N. J. Long, *Dalton Trans.* **2013**, *42*, 2813–2816.
- [8] a) *Comprehensive Coordination Chemistry, Vol. 5* (Eds: G. Wilkinson, R. D. Gillard, J. A. McCleverty), Pergamon Press, Oxford, **1989**; b) E. M. Njogu, B. Omondi, V. O. Nyamori, *J. Coord. Chem.* **2015**, *68*, 3389–3431.
- [9] a) B. Cordero, V. Gómez, A. E. Platero-Prats, M. Revés, J. Echeverría, E. Cremades, F. Barragán, S. Alvarez, *Dalton Trans.* **2008**, 2832–2838; b) M. Streitberger, A. Schmied, R. Hoy, E. Hey-Hawkins, *Dalton Trans.* **2016**, *45*, 11644–11649.
- [10] F. H. Allen, *Acta Crystallogr. Sect. B* **2002**, *58*, 380–388.
- [11] a) M. N. I. Khan, R. J. Staples, C. King, J. P. Fackler, R. E. P. Winpenny, *Inorg. Chem.* **1993**, *32*, 5800–5807; b) J. J. P. Fackler, Jr., J. M. Forward, T. Grant, R. J. Staples, *J. Mol. Struct.* **1998**, *470*, 151–160.
- [12] M. Sircoglou, S. Bontemps, G. Bouhadir, N. Saffon, K. Miqueu, W. Gu, M. Mercy, C.-H. Chen, B. M. Foxman, L. Maron, O. V. Ozerov, D. Bourissou, *J. Am. Chem. Soc.* **2008**, *130*, 16729–16738.
- [13] M.-E. Moret, L. Zhang, J. C. Peters, *J. Am. Chem. Soc.* **2013**, *135*, 3792–3795.
- [14] R. T. Stibrany, C. Zhang, T. J. Emge, H. J. Schugar, J. A. Potenza, S. Knapp, *Inorg. Chem.* **2006**, *45*, 9713–9720.
- [15] a) W.-H. Chan, K.-K. Cheung, T. C. W. Mak, C.-M. Che, *J. Chem. Soc. Dalton Trans.* **1998**, 873–874; b) V. J. Catalano, S. J. Horner, *Inorg. Chem.* **2003**, *42*, 8430–8438.
- [16] A. Dolmella, G. Bandoli, *Coord. Chem. Rev.* **2000**, *209*, 161–196.
- [17] I. Caracelli, J. Zukerman-Schpector, E. R. T. Tiekink, *Gold Bull.* **2013**, *46*, 81–89.
- [18] a) E. Herrero-Gómez, C. Nieto-Oberhuber, S. López, J. Bene tBuchholz, A. M. Echavarren, *Angew. Chem. Int. Ed.* **2006**, *45*, 5455–5459; *Angew. Chem.* **2006**, *118*, 5581–5585; b) P. Pérez-Galán, N. Delpont, E. Herrero-Gómez, F. Maseras, A. M. Echavarren, *Chem. Eur. J.* **2010**, *16*, 5324–5332; c) A. M. Wright, B. J. Irving, G. Wu, A. J. H. M. Meijer, T. W. Hayton, *Angew. Chem. Int. Ed.* **2015**, *54*, 3088–3091; *Angew. Chem.* **2015**, *127*, 3131–3134.
- [19] T. J. Mooibroek, P. Gamez, *Inorg. Chim. Acta* **2007**, *360*, 381–404.
- [20] a) S. Demeshko, S. Dechert, F. Meyer, *J. Am. Chem. Soc.* **2004**, *126*, 4508–4509; b) T. J. Mooibroek, C. A. Black, P. Gamez, J. Reedijk, *Cryst. Growth Des.* **2008**, *8*, 1082–1093; c) J. S. Costa, A. G. Castro, R. Pievo, O. Roubeau, B. Modéc, B. Kozlevčar, S. J. Teat, P. Gamez, J. Reedijk, *CrysEngComm* **2010**, *12*, 3057.
- [21] a) G. Garau, A. Frontera, D. Quiñero, P. Ballester, A. Costa, P. M. Deyà, *J. Phys. Chem. A* **2004**, *108*, 9423–9427; b) D. Quiñero, C. Garau, A. Frontera, P. Ballester, A. Costa, P. M. Deyà, *J. Phys. Chem. A* **2005**, *109*, 4632–4637.
- [22] F. Almaloti, J. MacDougall, S. Hughes, M. M. Hasson, R. L. Jenkins, B. D. Ward, G. J. Tizzard, S. J. Coles, D. W. Williams, S. Bamford, I. A. Fallis, A. Dervisi, *Dalton Trans.* **2013**, *42*, 12370–12380.
- [23] B. Therrien, G. Süß-Fink, P. Govindaswamy, A. K. Renfrew, P. J. Dyson, *Angew. Chem. Int. Ed.* **2008**, *47*, 3773–3776; *Angew. Chem.* **2008**, *120*, 3833–3836.
- [24] K. Ono, M. Yoshizawa, M. Akita, T. Kato, Y. Tsunobuchi, S.-I. Ohkoshi, M. Fujita, *J. Am. Chem. Soc.* **2009**, *131*, 2782–2783.
- [25] D. M. P. Mingos, T. E. Müller, *J. Organomet. Chem.* **1995**, *500*, 251–259.
- [26] G. Wu, R. E. Wasylshen, *Inorg. Chem.* **1996**, *35*, 3113–3116.
- [27] R. Corberán, S. Marrot, N. Dellus, N. Merceron-Saffon, T. Kato, E. Peris, A. Baceiredo, *Organometallics* **2009**, *28*, 326–330.
- [28] a) J. V. Hanna, R. D. Hart, P. C. Healy, B. W. Skelton, A. H. White, *J. Chem. Soc. Dalton Trans.* **1998**, 2321–2326; b) J. H. Nelson, *Concepts Magn. Reson.* **2002**, *14*, 19–78; c) F. D. Sokolov, M. G. Babashkina, F. Fayon, A. I. Rakhmatullin, D. A. Safin, T. Pape, F. Ekkehardt Hahn, *J. Organomet. Chem.* **2009**, *694*, 167–172.

- [29] a) D. A. Knight, S. W. Keller, *J. Chem. Crystallogr.* **2006**, *36*, 531–542; b) L. Chen, S. Deng, Q. Jin, P. Li, R. Wang, *Inorg. Chim. Acta* **2009**, *362*, 5224–5230; c) P. Štěpnička, I. Císařová, *Dalton Trans.* **2013**, *42*, 3373–3389; d) B. J. Barrett, V. M. Iluc, *Inorg. Chem.* **2014**, *53*, 7248–7259.
- [30] a) A. Báez-Castro, J. Baldenebro-López, A. Cruz-Enríquez, H. Höpfl, D. Glossman-Mitnik, M.-S. Valentin, M. Parra-Hake, J. J. Campos-Gaxiola, *RSC Adv.* **2014**, *4*, 42624–42631; b) S. Keller, A. Prescimone, E. C. Constable, C. E. Housecroft, *Polyhedron* **2016**, *116*, 3–11; c) A. Báez-Castro, J. Baldenebro-López, A. Cruz-Enríquez, H. Höpfl, D. Glossman-Mitnik, V. Miranda-Soto, M. Parra-Hake, E. Reynoso-Soto, J. J. Campos-Gaxiola, *Inorg. Chim. Acta* **2017**, *466*, 486–496.
- [31] a) D. A. Durfey, R. U. Kirss, C. Frommen, W. Feighery, *Inorg. Chem.* **2000**, *39*, 3506–3514; b) F. Barrière, R. U. Kirss, W. E. Geiger, *Organometallics* **2005**, *24*, 48–52; c) M. J. Verschoor-Kirss, O. Hendricks, C. M. Verschoor, R. Conry, R. U. Kirss, *Inorg. Chim. Acta* **2016**, *450*, 30–38.
- [32] P. H. Rieger, *Electrochemistry*, 2nd ed., Springer, Dordrecht, **1994**.
- [33] a) H. B. Gray, Y. S. Sohn, N. Hendrickson, *J. Am. Chem. Soc.* **1971**, *93*, 3603–3612; b) D. M. Duggan, D. N. Hendrickson, *Inorg. Chem.* **1975**, *14*, 955–970; c) S. Hartmann, R. F. Winter, B. M. Brunner, B. Sarkar, A. Knödler, I. Hartenbach, *Eur. J. Inorg. Chem.* **2003**, 876–891.
- [34] a) S. Yasui, K. Shioji, A. Ohno, *Tetrahedron Lett.* **1994**, *35*, 2695–2698; b) D. A. Khobragade, S. G. Mahamulkar, L. Pospíšil, I. Císařová, L. Rulišek, U. Jahn, *Chem. Eur. J.* **2012**, *18*, 12267–12277; c) K. D. Reichl, D. H. Ess, A. T. Radosevich, *J. Am. Chem. Soc.* **2013**, *135*, 9354–9357.

Manuscript received: January 15, 2020

Accepted manuscript online: February 5, 2020

Version of record online: April 22, 2020